Proceedings of the 11th World Congress on Mechanical, Chemical, and Material Engineering (MCM'25)

Paris, France - August, 2025 Paper No. ICMIE 195 DOI: 10.11159/icmie25.195

Effect of Electrochemical Machining Time on Burr Removal Efficiency under Constant Electrolyte and Electrical Conditions

Gülçin Deniz¹

1 Bursa Uludag University, Environmental Engineering / Doğu Pres R&D Center MinareliçavuşOSB No:8 16440, Bursa, Turkiye gulcindeniz@dogupres.com

Abstract - Electrochemical machining has become the preferred precise deburring method for injector components with complex geometries that were machined by conventional techniques. However, the effect of machining time on deburring performance under fixed process conditions is still insufficiently explored in the literature. This study quantitatively evaluates the deburring efficiency of two exposure times—6 s and 12 s—while all electrical and electrolyte parameters are kept constant (80 A, 40 V, 125 mS cm⁻¹ NaNO₃, pH 7.6, 22 °C, 85 L h⁻¹). Ten specimens made of X_4 CrNiMo16-5-1 stainless steel (five per time level) were processed, and the outcomes were analysed by digital microscopy and high-precision weighing. Extending the machining time from 6 s to 12 s increased total mass removal (mean Δ m: 0.0044 g \rightarrow 0.0060 g) and produced a statistically significant reduction in burr area (55 % vs 146 %; p = 0.023). Conversely, the instantaneous material-removal rate decreased slightly (0.60 g s⁻¹ \rightarrow 0.49 g s⁻¹). Short-duration runs exhibited high variability, including occasional burr growth—whereas longer exposures yielded more consistent and reliable results. These findings reveal a clear time–efficiency trade-off in electrochemical machining: moderate machining intervals strike an optimal balance between quality and productivity. The results provide a quantitative foundation for adaptive control strategies, cathode-design improvements, and simulation-based optimization in precision deburring applications.

Keywords: electrochemical machining; burr removal efficiency; machining time; material removal rate; process optimization

1. Introduction

One of the prominent industrial use cases of electrochemical machining (ECM) is in the fabrication of injector components for internal combustion engines, where tight geometric tolerances and clean joint transitions are critical for both performance and durability. ECM is a well-established non-traditional machining process that utilizes electrochemical principles to remove material from electrically conductive workpieces. It is especially suitable for machining hard-to-cut materials, such as nickel-based superalloys, titanium alloys, and high-strength steels, which pose significant challenges for conventional machining methods due to tool wear, residual stress, and thermal damage [1], [2]. Unlike subtractive processes based on mechanical forces, ECM is a contactless method that operates through anodic dissolution—wherein the workpiece acts as the anode, the tool as the cathode, and the inter-electrode space is filled with a conductive electrolyte. When a direct current is applied across the electrodes, metal ions dissolve from the workpiece into the electrolyte, achieving precise material removal without inducing heat-affected zones, mechanical deformation, or tool wear [3].

The unique capabilities of ECM, such as the ability to generate burr-free surfaces, maintain dimensional accuracy, and machine complex geometries, make it increasingly valuable in high-precision applications across aerospace, medical, defence, and automotive industries [2], [4]. The influence of the electrochemical machining process parameters like current, voltage, electrolyte concentration, feed rate, gap and flow rate were considered as the input parameters. The influence of the ECM process parameters current, voltage, electrolyte concentration, feed rate, gap and flow rate on the predominant output parameters material removal rate, surface roughness and radial overcut were also analysed. The output responses are the material removal rate (MRR), the surface roughness (SR) and the radial overcut (ROC). The study shows that the dominant output parameter MRR was directly proportional to the input parameters current, voltage and feed rate [5]. Conventional turning or milling methods often leave behind undesirable burr or fail to adequately machine the inner radius of intricate features, necessitating secondary processes that increase production time and cost. Deburring, especially in precision parts

with intricate features, has traditionally relied on mechanical or manual methods, which are time-consuming and prone to inconsistency. ECM, on the other hand, offers an efficient and scalable approach for high-accuracy burr removal, particularly in microstructural cavities and edges where tool access is limited. ECM is a complex process involving electrochemical reactions at the cathode, flow of electrolyte in the electrode gap and distribution of current density between electrodes. Electrochemical reactions lead to the generation of hydrogen gas bubbles, adversely affecting the flow pattern and conductivity of electrolyte which in turn causes changes in velocity profile, pressure distribution, generation of eddies, temperature of electrolyte the combined effect of which adversely affect MRR, surface finish and dimensional accuracy [6], [7].

Due to high wear resistance and hardness of this material, it cannot be machine with conventional machining process. Among non-conventional machining methods ECM is a potential process which is useful for machining such difficult-to-cut electrically conductive materials. ECM has been extensively used in machining of hard-to cut materials such as titanium, stainless steel, high-strength temperature resistant alloys, ceramics, refractories, fiber rein forced composites, super alloys etc. which are not suitable to be machined by the conventional machining processes because of their high hardness, strength, brittleness, toughness and low machinability properties [8]. Time plays a crucial role in determining the extent of electrochemical dissolution, particularly in regions with geometric discontinuities, such as burr roots and sharp internal corners. Increased machining time generally leads to deeper material penetration and more complete burr elimination, though excessive durations may risk overcut or loss of dimensional fidelity [9].

A comprehensive survey of the literature confirms that recent advances in ECM—spanning theory, experimentation, modelling and optimization—have progressively shifted from macro- to micro-scale applications, with vibration-assisted ECM emerging as the most mature auxiliary technique relative to alternatives such as abrasive-jet, magnetic-assisted or laser-assisted variants; additional progress in jet-assisted and wire ECM is also summarized, together with key research gaps and future directions [10]. Advanced studies using pulsed ECM systems have emphasized the importance of time-dependent control variables, such as pulse duration and duty cycle, to improve local dissolution accuracy [11]. However, most of these investigations have been carried out under variable electrical or electrolyte conditions, making it difficult to isolate the pure effect of machining time. Moreover, recent literature calls for simplified, cost-effective, and experimental validation approaches to model and optimize time-sensitive responses in ECM, especially for industrial-scale applications [2], [5].

In this context, the present study aims to isolate and quantify the effect of machining time on burr removal efficiency under constant electrical and electrolyte conditions. A sodium nitrate-based electrolyte with a fixed conductivity of 125 mS/cm, voltage of 40 V, current of 80 A, pH of 7.6, and flow rate of 85 L/h was used across all tests. The only varying parameter was the machining time, applied at two levels: 6 seconds and 12 seconds. Ten samples were processed (five per group), and changes in burr geometry and material removal were evaluated. The findings offer insight into the time-dependent behaviour of ECM in localized deburring and serve as a baseline for future developments in cathode design, process simulation, and deburring optimization.

2. Materials and Methods

2.1. Electrochemical Machining Setup

The experimental study was carried out using a custom-designed ECM system. The core components of the setup include a programmable direct current (DC) power supply, a cathode (tool electrode), an anode (workpiece), a recirculating electrolyte tank with high-pressure pump, and control modules for flow rate, temperature, and voltage monitoring (Figure 2.1). The tool (cathode) and workpiece (anode) are positioned with a controlled inter-electrode gap of approximately 0.2 mm. When DC voltage is applied, electrochemical reactions occur on the anodic surface, resulting in metal dissolution and burr removal.

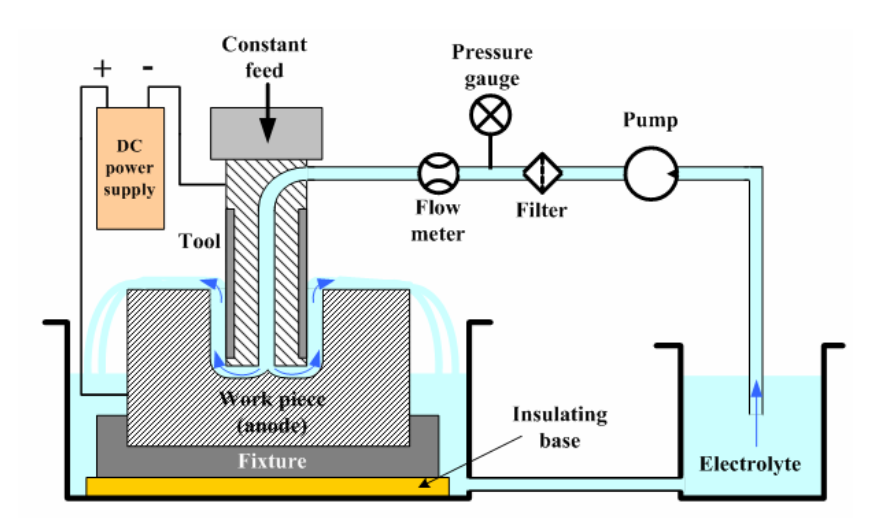


Figure 2.1. Schematic representation of the electrochemical machining (ECM) setup used in the experiments, showing the DC power supply, cathode (tool), anode (workpiece), electrolyte circulation system, and control units for temperature, pH, and conductivity.

The electrolyte is continuously circulated between the electrodes at a constant pressure and temperature to ensure stable reaction kinetics and uniform dissolution. The system includes integrated sensors for real-time monitoring of electrolyte temperature (± 0.5 °C accuracy), pH stability, and electrical conductivity. The non-contact nature of ECM eliminates mechanical stresses, tool wear, and burr redeposition, allowing for highly controlled surface shaping, particularly in confined and geometrically complex regions [1], [2].

2.2. Workpiece and Tool Materials

The workpieces used in this study were fabricated from X_4 CrNiMo16-5-1 stainless steel (1.4418 according to EN standard), a martensitic precipitation-hardened alloy commonly employed in high-performance hydraulic and injection system components. This steel grade offers a favorable combination of high tensile strength, excellent corrosion resistance, and adequate electrical conductivity, making it suitable for electrochemical machining applications. The samples were prepared in cylindrical form with an external hole diameter of 3.5 mm.

The tool electrode (cathode) was manufactured from AISI 316L stainless steel, annealed selected for its favorable combination of corrosion resistance, mechanical strength, and adequate electrical conductivity for ECM applications. Although 316L exhibits lower electrical conductivity compared to copper, it provides greater dimensional stability and chemical inertness in aggressive electrolyte environments, making it suitable for repeated use and precision-controlled material removal. The electrode was fabricated as a cylindrical rod with a 3 mm diameter, identical to that of the workpiece, and carefully aligned with the burr-affected region. The workpiece contains a pre-drilled hole with a diameter of 3.5 mm, while the cathode is a cylindrical rod with a 3.0 mm diameter positioned concentrically inside the hole. The 0.25 mm radial gap ensures uniform electrolyte flow and controlled current density distribution along the inner burr region during electrochemical machining (Figure 2.2).

To ensure controlled current flow and minimize undesired lateral dissolution, only the front-facing surface of the cathode was left exposed. The remaining surfaces were coated with a chemically resistant insulating polymer, which confined the electric field to the target area. This partial insulation strategy promotes focused current density at the machining zone and improves burr removal performance by reducing the effect of stray currents and ensuring directional dissolution [4], [11].

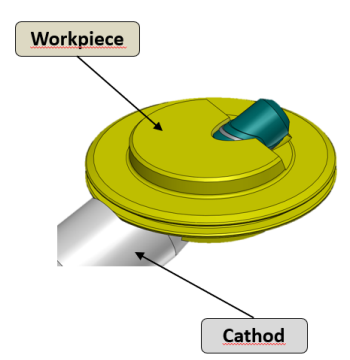


Figure 2.2. Schematic representation of the ECM setup showing the alignment between the cathode and workpiece.

2.3. Electrolyte Composition and Conditions

A water-based sodium nitrate (NaNO₃) solution was used as the electrolyte due to its chemical neutrality, high conductivity, and non-aggressive behaviour toward tool surfaces. The concentration was adjusted to achieve a measured conductivity of 125 mS/cm, which is representative of medium-strength electrolytes in ECM literature [5], [6].

Table 2.1. Constant Electrolyte and	Environmental Conditions	Used in ECM Experiments
-------------------------------------	--------------------------	-------------------------

Parameter	Value	Unit
pН	7.6	_
Temperature	22	°C
Flow Rate	85	L/h
Conductivity	125	mS/cm

The flow system ensured continuous agitation of the electrolyte through the machining gap, preventing local ion saturation and removing byproducts such as metal hydroxides and gas bubbles from the inter-electrode region [7]. Temperature stability was achieved using an external chiller and in-line heat exchanger, maintaining the reaction zone at ambient conditions.

2.4. Process Parameters and Experimental Design

To isolate the effect of machining time, all other process parameters were held constant throughout the study. The applied voltage was fixed at 40 V, and the output current was maintained at 80 A via a stabilized DC supply. The only variable was the duration of machining, applied at two discrete levels: 6 seconds and 12 seconds. The electrochemical machining experiments were conducted under strictly controlled process conditions to isolate the effect of machining time on burr removal. A constant voltage of 40 V and current of 80 A were applied throughout all trials. The electrolyte solution, based on sodium nitrate, was maintained at a conductivity of 125 mS/cm, with a pH of 7.6 and a stable temperature of 22 °C. The electrolyte was circulated at a fixed flow rate of 85 L/h to ensure uniform ion transport and efficient removal of reaction byproducts. Machining time was the only variable, applied at two discrete levels: 6 seconds and 12 seconds. These parameters ensured a consistent electrochemical environment for evaluating time-dependent effects on burr dissolution (Table 2.2).

Table 2.2. Electrochemical Machining Parameters Used in the Experiments

Parameter	Value	
Voltage	40 V	
Current	80 A	
Machining Time	6 s / 12 s	
Conductivity	125 mS/cm	
pН	7.6	
Temperature	22 °C	
Flow Rate	85 L/h	

A total of 10 samples were processed — 5 samples at each time level — to ensure statistical consistency. The burr geometries on the samples were pre-characterized using digital microscopy, and no further machining or finishing was applied after ECM treatment.

2.5. Evaluation and Measurement Methods

After ECM processing, each sample was cleaned, dried, and examined under a digital microscope (Leica M50) to measure changes in burr dimensions, including burr height and burr base width. The burr morphology, before and after ECM processing was examined using a Leica M50 stereo microscope, equipped with a 5:1 step-zoom system offering fixed magnification levels at 10×. This configuration enabled consistent and reproducible imaging of the burr regions under controlled optical conditions.

Additionally, weight loss of the samples was recorded using an analytical balance with 0.1 mg resolution to estimate the material removal during each trial. Burr Removal Efficiency (%) was calculated by comparing pre- and post-process. Material Removal Rate (MRR) was computed as the mass loss per unit time (g/s).

2.6 Data Analysis

The primary goal of the data analysis phase was to evaluate the effect of machining time on burr geometry and material removal under constant ECM conditions. A total of 10 samples were processed in two groups: five samples were machined for 6 seconds and five samples for 12 seconds, while all other process parameters were held constant. Quantitative measurements were taken for burr width, burr height, burr cross-sectional area, and total mass loss (in grams) both before and after ECM. Additionally, a derived R-value, representing a combined burr severity index, was calculated to aid in comparative evaluation. Burr dimensions were measured using a high-resolution digital microscope (Leica M50) at magnification 10×. The burr cross-sectional area was computed using the formula for a triangular shape based on measured width and height. Mass loss was obtained from high-precision balance readings, allowing the estimation of material removal rate (MRR). This section quantifies the influence of machining time (6 s vs 12 s) on burr geometry and material removal by means of an independent-samples t-test. Ten specimens were processed under identical ECM parameters: five were machined for 6 s and five for 12 s, while current (80 A), voltage (40 V), electrolyte conductivity (125 mS cm⁻¹), pH 7.6, temperature 22 °C, and flow rate 85 L h⁻¹ remained constant.

Burr dimensions were recorded with a Leica M50 digital microscope at 10× magnification. Assuming a triangular profile, burr cross-sectional area was calculated as (1).

$$A = \frac{1}{2} (width) \times (height) \tag{1}$$

Mass loss (Δm) was obtained from pre- and post-machining weights measured with a 0.1 mg analytical balance. Instantaneous material-removal rate (MRR) was computed as (2).

$$MRR = \frac{\Delta m}{t_{mach}}$$
 (2)

(g s⁻¹), where t_mach equals 6 s or 12 s. Burr-area reduction (%) was determined via (3)

$$\% \Delta A = \frac{A_{before} - A_{after}}{A_{before}} x 100$$
 (3)

Normality was confirmed with the Shapiro–Wilk test (p > 0.10); therefore, group means were compared using an independent-samples t-test with Welch correction (α = 0.05). Calculations were performed in Python (SciPy 1.10). The results of the data analysis are shown at Table 2.3.

 $12s (n = 5) Mean \pm SD$ Metric 6s (n=5) Mean \pm SD $t (df \approx 7)$ Mass loss Δm (g) 0.0044 ± 0.0023 0.0060 ± 0.0048 1.03 0.34 Instantaneous MRR (g s⁻¹) 0.60 ± 0.29 0.49 ± 0.39 -0.520.62 **Burr-area reduction (%)** -146 ± 163 $+55 \pm 30$ 2.71 0.023

Table 2.3. Table of *t test* results.

These results provide quantitative evidence that machining time is critical—above all—for the consistency of burr elimination under otherwise fixed ECM conditions. Although extending pulse duration did not significantly increase total mass removal or instantaneous MRR, it yielded a statistically significant (p < 0.05) improvement in burr-area reduction. Consequently, even under constant electrical and electrolyte settings, pulse length remains a key parameter for reliable deburring. These controlled findings can serve as benchmark data for future simulation validation and cathode-design optimization.

3. Results

The effect of machining time on burr removal efficiency under constant ECM parameters was evaluated through quantitative comparison of burr geometry and mass loss before and after machining. The experiments were grouped according to machining duration: 6 seconds (Samples 1–5) and 12 seconds (Samples 6–10), with all other parameters kept constant (80 A, 40 V, conductivity 125 mS/cm, pH 7.6, 22 °C, 85 L/h).

3.1 Material Removal

Material removal was assessed by calculating the weight difference (gram loss) before and after ECM for each sample. In the 6-second group, the mass loss ranged from 0.0010 g to 0.0070 g, whereas the 12-second group exhibited a wider range from 0.0010 g to 0.0110 g. The highest material removal was recorded in Sample 8 (0.0110 g), corresponding to a calculated MRR of 0.9166 g/s, whereas the lowest value was 0.0833 g/s in Samples 6 and 7. Overall, a general increase in material removal rate was observed with longer machining times, although the variation among samples indicates that burr morphology and local current density likely influenced the dissolution dynamics.

3.2 Burr Geometry Reduction

Burr width and height differences were used to compute the change in burr cross-sectional area. Samples in the 6-second group exhibited burr width reductions ranging from -0.0723 mm to -0.1364 mm and burr height reductions between -0.0387 mm and -0.0516 mm, with corresponding area reductions between 0.0064 mm² and 0.0109 mm².

In contrast, samples in the 12-second group showed mixed results. For example:

- -Sample 6 presented a moderate area reduction (0.0287 mm²),
- -Sample 7 showed 0.0371 mm² area reduction,
- -Sample 10, despite having the largest initial burr, resulted in the highest area reduction (0.0798 mm²),
- -while Sample 9 displayed positive burr growth in both width and height, indicating a possible local redeposition or insufficient exposure.

For example: Sample 6 presented a moderate area reduction (0.0287 mm²), Sample 7 showed 0.0371 mm² area reduction, Sample 10, despite having the largest initial burr, resulted in the highest area reduction (0.0798 mm²), while Sample 9 displayed positive burr growth in both width and height, indicating a possible local redeposition or insufficient exposure (Figure 3.1).

These variations highlight that although increased machining time generally supports improved burr removal, the initial burr volume and spatial orientation relative to the tool play a significant role in localized dissolution efficiency.

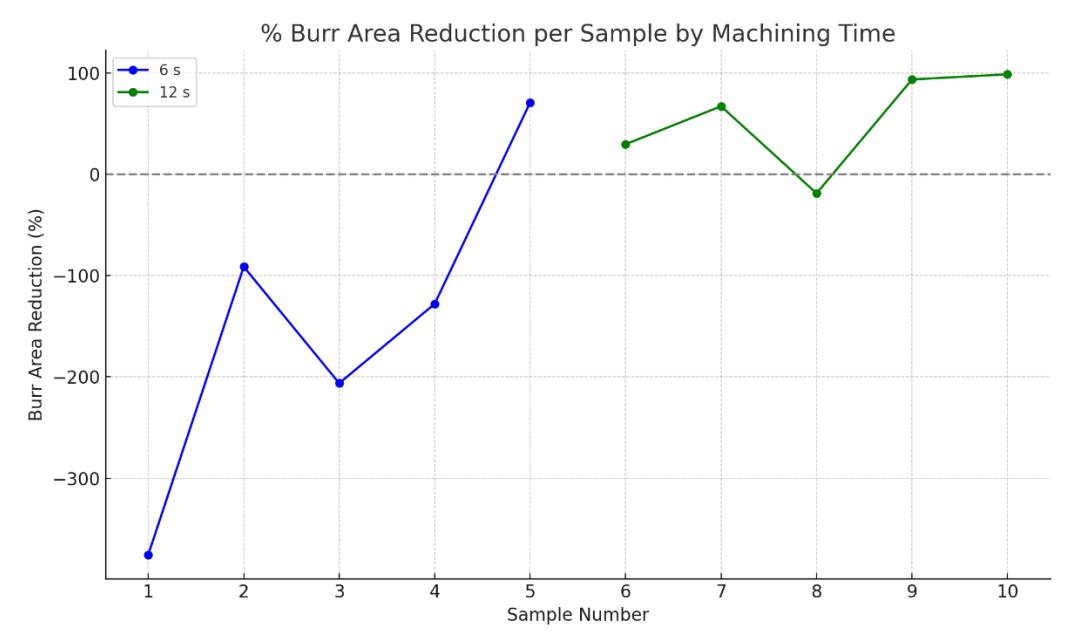


Figure 3.1. Percentage reduction in burr area for each ECM-processed sample, categorized by machining time (6 s and 12 s). Blue line represents the 6-second group (Samples 1–5), while the green line represents the 12-second group (Samples 6–10). Negative values reflect potential burr growth or measurement variation.

3.3 Calculated Burr Areas and Pattern Analysis

The computed burr areas (from width and height differences) confirm the impact of machining time. The average calculated burr area in the 6-second group was approximately 0.0153 mm², while the 12-second group achieved a slightly higher average of 0.0269 mm² due to a few high-outlier samples (e.g., Sample 10). However, when normalized per second of machining time, the efficiency of burr reduction per unit time was higher in shorter duration trials, suggesting diminishing returns at extended durations unless current focusing or cathode design is further optimized.

3.4 Comparative Evaluation of the 6 s and 12 s Runs

Table 3.1 make it possible to contrast the two exposure times in terms of material removal, residual-burr index and burrarea-reduction behaviour.

-Total vs. Instantaneous Productivity

Extending machining time from 6 s to 12 s increases total mass removed but diminishes the material-removal rate per second. This confirms a time-efficiency trade-off: once the diffusion layer stabilizes and the inter-electrode gap saturates with metal ions, the marginal removal rate declines.

-Process Robustness

The 6-second series show large sample-to-sample swings, including four instances of negative burr-area reduction. Such variability is consistent with transient bubble entrapment or momentary shielding of the burr tip by partially detached debris. By contrast, all 12-second samples record positive burr reduction, and three exceed 50 %, demonstrating that longer exposure mitigates short-term instabilities and yields more reliable deburring.

Table 3.1. Table of Comparative evaluation of the 6 s and 12 s Runs ¹ Negative values denote apparent burr growth – a symptom of insufficient dissolution or measurement artefacts.

Metric	6 s (n = 5)	12 s (n = 5)	Observation
Weight loss, g	0.0044 ± 0.0023	0.0060 ± 0.0048	Longer runs remove \approx 36 % more mass on average, but with twice the scatter.
Instantaneous MRR, g s ⁻¹	0.60 ± 0.29	0.49 ± 0.39	Normalised to time, the short run is∼ 20 % more efficient.
Burr-area change (%), mean	highly variable $-146 \% \pm 163 \%^{1}$	predominately + 55 % ± 30 %	6 s runs oscillate between growth and removal; 12 s runs give consistently positive reduction.

The present study demonstrates that, even under rigorously controlled electrical and electrolyte conditions, machining time exerts a decisive influence on burr removal performance in ECM. Extending the process duration from 6 s to 12 s generally improved burr dissolution uniformity, yet this benefit must be weighed against a decline in instantaneous removal efficiency (g/s). This inverse relationship between total burr reduction and material removal rate echoes findings in prior pulsed-ECM investigations, where prolonged exposure enhanced surface finishing at the expense of throughput [9], [11].

The pronounced variability observed in the 6-second group—highlighted by both negative and highly positive burr area changes—suggests that short-duration runs may be more susceptible to localized phenomena such as gas bubble entrapment, transient concentration gradients, and uneven current distribution. Such effects can momentarily block the electrolyte gap or concentrate current at sharp burr tips, leading to inconsistent dissolution. In contrast, the longer-duration group achieved more consistent, positive burr reductions, indicating that extended machining permits the reestablishment of stable diffusion layers and more uniform flushing of reaction byproducts [7].

However, the diminishing returns in burr removal per unit time beyond the initial few seconds point to the onset of mass-transport limitations and electrolyte saturation near the machining zone. As the local ion concentration shifts and gas evolution intensifies, the net dissolution rate plateaus. This behaviour underscores the necessity of optimizing machining time to balance productivity with burr-free quality—prolonged runs yield incremental gains in burr removal but at disproportionately lower MRR. From a practical standpoint, these results inform process planners that a moderate machining interval (e.g., 8–10 s) may achieve a favorable compromise between reliable burr elimination and acceptable cycle times. Furthermore, the data underlines the potential of adaptive control strategies—such as real-time monitoring of current fluctuations or electrolyte properties—to dynamically adjust machining time and mitigate the impact of localized instabilities.

The line graph in Figure 3.1 illustrates individual sample responses in terms of burr area reduction as a function of machining time. The 6-second group (Samples 1–5) showed a wide range of outcomes, including several cases (e.g., Samples

1–3) where burr area appeared to increase after machining. These anomalies may be attributed to insufficient exposure time for effective electrochemical dissolution, or to repositioning of partially detached burrs within the measurement region. In contrast, the 12-second group (Samples 6–10) demonstrated more consistent and positive reductions in burr area, with Sample 10 exhibiting an exceptionally high reduction rate exceeding 99%.

The presence of negative or marginal gains in the shorter-duration group underscores the sensitivity of ECM performance to exposure time, especially when local burr morphology or electrolyte flow is non-uniform. Longer machining durations appear to stabilize electrochemical interactions, allowing for more complete flushing of byproducts and better current density distribution across the burr interface. These results reinforce the conclusion that machining time is a critical parameter for ensuring both the effectiveness and reliability of burr removal in ECM. Finally, the insights gained here provide critical input parameters for future simulation models and cathode design iterations.

4. Conclusion

This study investigated the effect of machining time on burr removal efficiency during ECM under constant electrical and electrolyte conditions. By systematically varying only the machining duration (6 s and 12 s), the isolated impact of time on burr geometry and material removal was quantitatively assessed. The results demonstrated that longer machining times generally led to greater burr reduction and more consistent dissolution behaviour. The 12-second trials showed higher total burr area reduction and improved surface uniformity, particularly in samples with initially large burrs. However, when normalized by time, the 6-second group exhibited higher instantaneous material removal rates (g/s), indicating a decline in efficiency beyond certain durations. These findings point to a time-efficiency trade-off inherent to ECM and highlight the importance of optimizing process duration for both quality and productivity.

Furthermore, reinforces the value of incorporating time-sensitive control mechanisms in future ECM systems. In conclusion, machining time is a critical parameter influencing burr removal outcomes in ECM, even under fully controlled conditions. The data presented here provide a foundation for further exploration of adaptive control strategies, cathode tool design enhancements, and process simulation models aimed at achieving precision deburring in complex components.

Acknowledgements

The author gratefully acknowledges the support of Doğu Pres R&D Center for providing the experimental facilities and funding for this research. This study would not have been possible without their valuable contributions.

References

- [1] Jain, V. K., & Jain, P. K. Advanced machining processes. Allied Publishers, 2007.
- [2] Defanti, S., Tirillò, J., Cicala, G., Sarasini, F., & Santulli, C. The electrochemical machining of difficult-to-cut materials: A comprehensive review. *Micromachines*, 2020, 11(11), 1050. https://doi.org/10.3390/mi11111050
- [3] Schulze, H. P. The electrochemical machining process—Theoretical fundamentals and applications. Materialwissenschaft und Werkstofftechnik, 2009, 40(10), 783–791. https://doi.org/10.1002/mawe.200900480
- [4] Krauss, H., Rebelo, N., & Dambon, O. Investigations on the electrochemical machining of microstructures. Production Engineering, 2007, 1(3), 233–238. https://doi.org/10.1007/s11740-007-0037-y
- [5] Mariapushpam, A., & Ravindran, D. Performance evaluation of electrolyte in ECM process using taguchi method. *International Journal of Mechanical Engineering and Technology*, 2016, 7(6), 207–213.
- [6] Galati, M., Caggiano, A., & Gagliardi, F. A review on ECM technology: Process characteristics and recent developments in tool design and performance. Journal of Manufacturing Processes, 2022, 79, 361–380. https://doi.org/10.1016/j.jmapro.2022.04.036
- [7] Nayak, D., Mahapatra, S. S., & Panda, A. Investigations on the effects of process parameters on performance in ECM of EN31 steel. Procedia Technology, 2016, 25, 1039–1046. https://doi.org/10.1016/j.protcy.2016.08.241

- [8] Teimouri, R., & Sohrabpoor, H. Modeling and multi-response optimization of electrochemical machining parameters for surface quality improvement. Journal of Manufacturing Processes, 2013, 15(4), 460–467. https://doi.org/10.1016/j.jmapro.2013.07.004
- [9] Zindani, D., Shunmugam, M. S., & Chakraborty, S. Modeling and optimization of electrochemical machining of titanium using grey relational analysis. Materials and Manufacturing Processes, 2019, 34(7), 769–776. https://doi.org/10.1080/10426914.2019.1593887
- [10] Painuly, M., Singh, R. P., & Trehan, R. Electrochemical machining and allied processes: a comprehensive review. Journal of Solid-State Electrochemistry, 2023, 27(12), 3189-3256. https://doi.org/10.1007/s10008-023-05610-x
- [11] Holstein, N., Schulze, H. P., & Langemann, M. Simulation of ECM processes with pulsed voltage. International Journal of Machine Tools and Manufacture, 2011, 51(6), 528–535. https://doi.org/10.1016/j.ijmachtools.2011.03.006